nature nanotechnology

ARTICLES

PUBLISHED ONLINE: 1 FEBRUARY 2009 | DOI: 10.1038/NNANO.2008.404

Engineering the coupling between molecular spin qubits by coordination chemistry

Grigore A. Timco[1], Stefano Carretta[2], Filippo Troiani[3], Floriana Tuna[1], Robin J. Pritchard[1], Christopher A. Muryn[1], Eric J. L. McInnes[1], Alberto Ghirri[3,4], Andrea Candini[3], Paolo Santini[2], Giuseppe Amoretti[2], Marco Affronte[3,4]* and Richard E. P. Winpenny[1]*

The ability to assemble weakly interacting subsystems is a prerequisite for implementing quantum information processing and generating controlled entanglement. In recent years, molecular nanomagnets have been proposed as suitable candidates for qubit encoding and manipulation. In particular, antiferromagnetic Cr_7Ni rings behave as effective spin-1/2 systems at low temperature and show long decoherence times. Here, we show that these rings can be chemically linked to each other and that the coupling between their spins can be tuned by choosing the linker. We also present calculations that demonstrate how realistic microwave pulse sequences could be used to generate maximally entangled states in such molecules.

Entanglement is a genuine quantum phenomenon in which the states of two or more quantum systems are correlated so that they cannot be described independently from one another. The controlled generation of entanglement is a key requirement for implementing quantum information processing (QIP)[1]. In this regard, the system has to be composed of a collection of N well-defined, effective two-level systems (qubits). So far, maximal entanglement in multipartite systems ($N > 2$) has been generated with photons[2,3] and trapped ions[4,5]. Analogous demonstrations have also been achieved in mesoscopic systems for the bipartite ($N = 2$) case[6,7].

The spin of a single electron can be regarded as the prototypical two-level system. However, the qubit encoded in a spin cluster[8–13] can be individually addressed through local fields, thanks to the larger size of the logical unit[13,14]. Single molecules with magnetic features represent a rich class of spin clusters. They generally consist of an inorganic core with a variable number of magnetic ions, linked by superexchange bridges and surrounded by a shell of organic ligands[14]. Despite this structural complexity, at low temperatures most molecular spin clusters behave as effective few-level systems. In addition, the electron spin degrees of freedom can be sufficiently decoupled from the environment (for example, the nuclei) to give long decoherence times[15] and allow the observation of forced oscillations[16]. Apart from these single molecule properties, the presence of a magnetic coupling between pairs of molecular spin clusters is required to perform QIP. Such coupling has so far been demonstrated only in Mn_4 molecules[17,18]; however, these have high spin and large anisotropy, and the coupling is not easy to tailor, which potentially limits their relevance to QIP applications[19].

Here, we focus on a specific class of molecular spin clusters, which contain one Ni^{2+} and seven Cr^{3+} centres, arranged in an octagonal ring and held together by fluoride and carboxylate ligands[20]. Such rings have recently been characterized through a variety of experimental techniques[21–23], and as a result of antiferromagnetic (AF) coupling between neighbouring ions, they possess an $S = 1/2$ ground state. At sufficiently low temperatures, excited-state multiplets are unoccupied, but represent a potential resource for the implementation of two-qubit quantum gates if deliberately involved[24]. Relatively long decoherence times have been measured and can be lengthened significantly by rational chemical modifications[16,25]. It is also possible to attach Cr_7Ni rings to surfaces[26], which could enable individual manipulation. These properties make a Cr_7Ni molecule suitable for qubit encoding and manipulation. As a further step, the coherent coupling between the spins of two such molecules is required.

Here, we show that this can be achieved with a high degree of flexibility and control, and without altering the structure and magnetic properties of the building blocks, by means of coordination chemistry. The synthetic procedure comprises three steps with relatively high yields. The system characterization is carried out through complementary experimental techniques (electron paramagnetic resonance (EPR), low-temperature specific heat and magnetic susceptibility measurements). We find that the intermolecular coupling is large enough to allow coherent multi-qubit dynamics and manipulation. Furthermore, we theoretically show that in the tripartite system consisting of two Cr_7Ni rings and a Cu ion, maximally entangled states can be generated in times much shorter than the expected decoherence time.

Chemical strategy

The synthesis of the ring, its functionalization, and the linking through a tuneable bridge takes three steps. In the first step, we synthesize Cr_7Ni rings[20] with 16 pivalate (O_2CCMe_3) ligands around the periphery. The chemical formula of the molecule is $[NH_2Pr_2][Cr_7NiF_8(O_2CCMe_3)_{16}]$ (**1**) (Pr is *n*-propyl) and it can be made in >70% yield. Each edge of the octagon is bridged by a fluoride and two carboxylate ligands. This version of the ring has a hydrocarbon exterior that needs to be chemically functionalized in order to introduce a linking group. In a second step, the AF-ring is reacted with iso-nicotinic acid in boiling *n*-propanol.

[1]The Lewis Magnetism Laboratory, School of Chemistry, The University of Manchester, Oxford Road, Manchester M13 9PL, UK, [2]Dipartimento di Fisica, Università di Parma, v. G.P. Usberti n. 7/A, 43100 Parma, Italy, [3]CNR-INFM-S3 National Research Centre, via G. Campi 213/A, 41100 Modena, Italy, [4]Dipartimento di Fisica, Università di Modena e Reggio Emilia, via G. Campi 213/A, 41100 Modena, Italy; *e-mail: marco.affronte@unimore.it; Richard.Winpenny@manchester.ac.uk

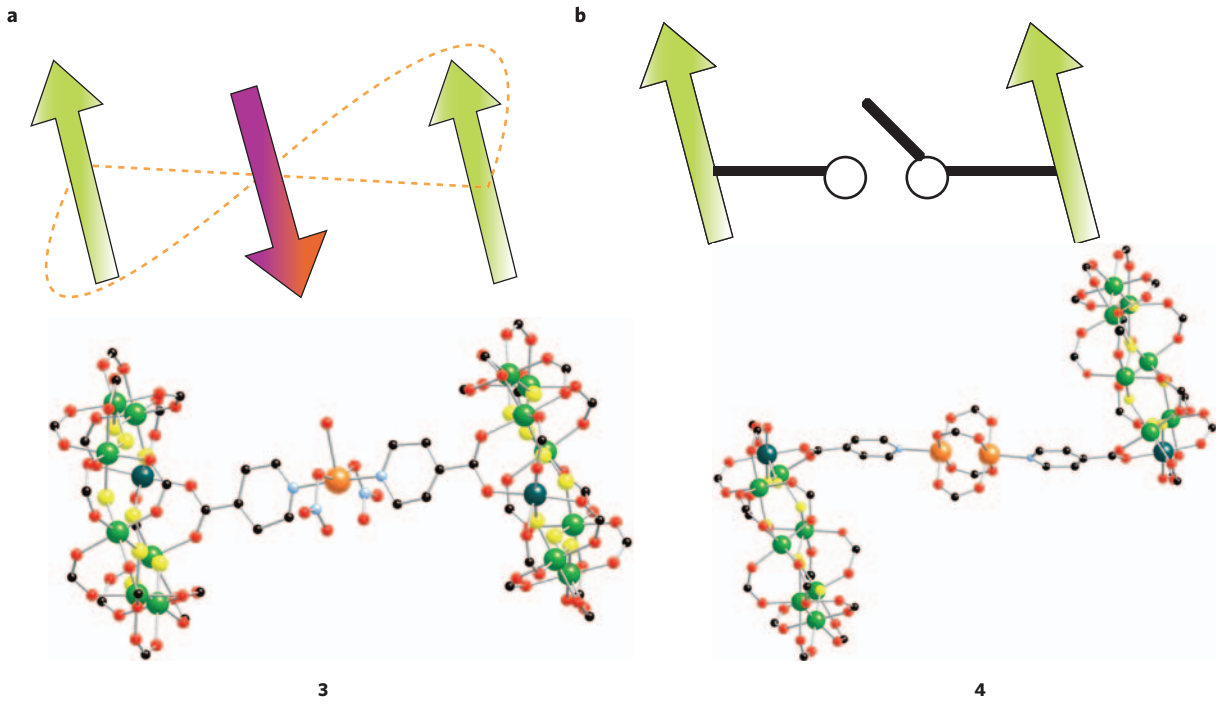

Figure 1 | Structures of the {Cr_7Ni}-link-{Cr_7Ni} molecules. a, Rings linked with a single Cu^{2+} centre (**3**) can be regarded as a three-qubit system. **b**, Rings coupled through a dimetallic link (**4**) implement two-qubit systems with switchable effective coupling. The coloured balls correspond to different atoms: Cr (light green), Ni (dark green), Cu (orange), O (red), N (yellow); tertiary butyl groups and NH_2Pr_2 are omitted for clarity.

A chromatographic separation follows, to give a functionalized compound, $[NH_2Pr_2][Cr_7NiF_8(O_2CCMe_3)_{15}(O_2CC_5H_4N)]$ (**2**), in 25% yield. The iso-nicotinate ligand provides a pyridine nitrogen group, which can be used to bind further metal centres, as required for inducing the magnetic coupling between rings. As substitution chemistry at nickel is much faster than that at chromium, the iso-nicotinate is introduced on one of the two edges of the octagon that contain the Ni^{2+} centre. In a third step, pairs of Cr_7Ni rings are coupled to each other through metallic links. This is done by mixing **2** with a suitable metal precursor in acetone or toluene; the linked complex forms with a yield approaching 80%, depending on the specific link used. Thus far, we have synthesized ring dimers with three distinct dimetallic links—$M_2(O_2CCMe_3)_4$, where $M = Cu^{2+}$, Ni^{2+} or $Ru^{2+}Ru^{3+}$—and two monometallic ones—either a single Cu^{2+} or Ni^{2+} centre. We stress that the metal centre in the link can be varied almost at will, as **2** shows the coordinating ability of a rather bulky pyridine ligand. This is appealing because different links can be chosen to change the way that the ring spins are electronically coupled and in principle meet the requirements of different QIP implementation schemes. Hereafter, we focus on two compounds: $\{[NH_2Pr_2][Cr_7NiF_8(O_2CCMe_3)_{15}(O_2CC_5H_4N)]\}_2[Cu(NO_3)_2(OH_2)]$ (**3**, in short $Cr_7Ni-Cu-Cr_7Ni$) and $\{[NH_2Pr_2][Cr_7NiF_8(O_2CCMe_3)_{15}(O_2CC_5H_4N)]\}_2[Cu_2(O_2CCMe_3)_4]$ (**4**, in short $Cr_7Ni-Cu_2-Cr_7Ni$); both are presented in Fig. 1.

Experimental determination of intermolecular coupling

A chemical link between pairs of Cr_7Ni rings does not guarantee magnetic coupling between their spins[27]. In order to establish whether such a coupling is present, we characterized different compounds by EPR, specific heat and magnetic susceptibility measurements. The results obtained with these complementary techniques support the picture of weakly interacting subsystems: first, the intra-ring magnetic couplings are preserved, that is, Cr_7Ni behaves as a building block; second, a weak magnetic coupling is established, which removes (in **3**) the degeneracy of the low-energy states.

Figure 2 shows the specific heat (C) for the $Cr_7Ni-Cu-Cr_7Ni$ (**3**) compound, as a function of the temperature (T). In order to highlight the effect of the inter-ring interaction, we compare the $C(T)$ curve with that obtained for two non-interacting rings. In zero field (panel **a**) the ground state of two non-interacting rings is fourfold degenerate and no feature appears in the low-temperature tail of $C(T)$ (blue crosses). The presence of an inter-ring coupling in **3** dramatically shows up in the specific heat through the Schottky anomaly appearing at $T < 1$ K (red circles). This feature reflects the magnetic coupling between the rings and the resulting zero field splitting of the ground multiplet of the $Cr_7Ni-Cu-Cr_7Ni$ system. Note that the Schottky anomaly is absent in **4** (see Supplementary Information, Fig. S2), which differs from **3** only by the metal M on the linker; this shows that the choice of such a linker allows us to control the effective interaction between the Cr_7Ni units. In high magnetic fields ($B_0 > 1$ T, panels **c**–**e**) the $C(T)$ curve of **3** is very close to that of the non-interacting case, demonstrating that the lowest-lying states of interacting and non-interacting rings essentially coincide. This shows that intra-molecular interactions and excitations of the Cr_7Ni molecule are preserved in **3**. The above picture is consistent with the results of the magnetic susceptibility (see Supplementary Information, Fig. S1) and is clearly corroborated by the powder EPR spectra reported in Fig. 3. The spectra of **3** at 5 K are completely different from those of two isolated Cr_7Ni rings plus a Cu^{2+} ion, while those of **2** and **4** are essentially identical to one another.

To interpret the experimental results, we first modelled the system through a microscopic approach. This also justifies the introduction of an effective three-spin model, which provides a more intuitive description of the EPR spectra and a suitable representation for discussing the generation of entangled states.

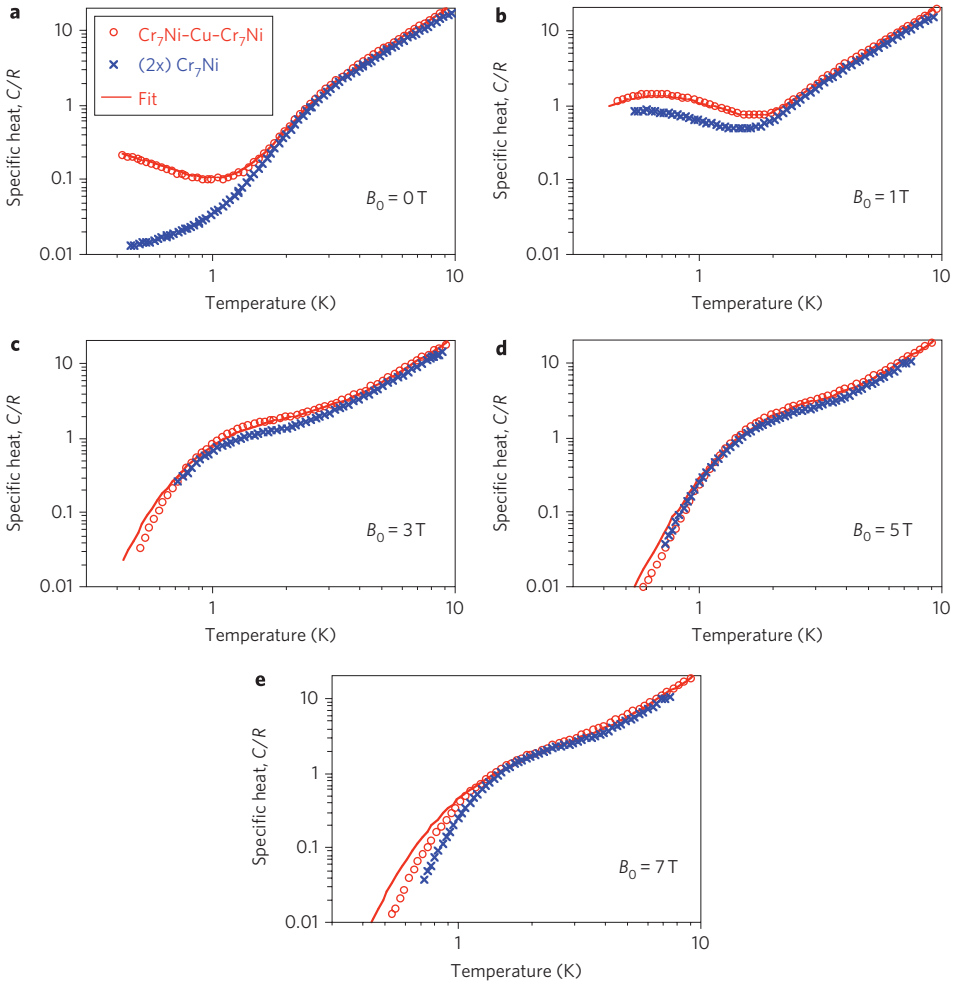

Figure 2 | Low-temperature specific heat *C* of linked and free Cr_7Ni rings. a–e, Measured $C(T)$ of Cr_7Ni–Cu–Cr_7Ni (open red circles) in units of $R = 8.314$ J mol^{-1} K^{-1}, for different values of the applied magnetic field B_0. The specific heat of uncoupled Cr_7Ni rings—multiplied by a factor 2—is reported for direct comparison (blue crosses, from ref. 11). Calculated specific heat (continuous red lines), with the intermolecular couplings J' as the only fitting parameters (intramolecular couplings are left unchanged with respect to the ones obtained in refs 21,22). In zero field (**a**), the Schottky anomaly at $T < 1$ K evidences the coupling between the Cr_7Ni rings and Cu^{2+} ion. For $B_0 > 1$ T (**c–e**) the energy levels of Cr_7Ni–Cu–Cr_7Ni are quite close to those of $(Cr_7Ni)_2$, so the two $C(T)$ curves almost overlap each other. At 1 T the Cu^{2+} also contributes to the specific heat of Cr_7Ni–Cu–Cr_7Ni; thus a difference in the $C(T)$ of isolated rings is still evident (**b**).

Our microscopic description of the different compounds is based on the following spin Hamiltonian:

$$H = H^{A} + H^{B} + H^{C} + H^{AC} + H^{BC} \qquad (1)$$

where the A, B and C subsystems correspond to the two rings and the magnetic link, respectively. As the rings preserve their internal structure (see Fig. 1), the terms H^A and H^B have the same expression as in non-interacting Cr_7Ni molecules[21,22]:

$$H^{A} = H^{B} = \sum_{i=1}^{8} J_i \vec{s}_i \cdot \vec{s}_{i+1} + \sum_{i=1}^{8} d_i s_{i,z}^2 + H_{dip} + \mu_B \vec{B} \cdot \sum_{i=1}^{8} \cdot \vec{g}_i \vec{s}_i, \qquad (2)$$

with z along the ring axis. The terms in the $H^{A/B}$ include isotropic exchange (J_i), axial crystal field (d_i) and dipole–dipole couplings (H_{dip}) between the eight individual spins $\vec{s}_i$. The last term describes the Zeeman coupling to the magnetic field. For compound **3**, the link comprises a single copper (II) centre:

$$H^{C} = \vec{B} \cdot \vec{\vec{g}}_{Cu} \cdot \vec{s}_{Cu}. \qquad (3)$$

The two link-ring coupling terms are given by

$$H^{AC} = H^{BC} = J' \vec{s}_{Cu} \cdot [\vec{s}_{Cr} + \vec{s}_{Ni}], \qquad (4)$$

where $\vec{s}_{Cr}$ and $\vec{s}_{Ni}$ correspond to $\vec{s}_1$ and $\vec{s}_8$, in their respective rings. The edge of the octagon bound to the Cu link contains a Ni and a Cr centre. Although the coupling of the Cu ion to Cr and Ni could in principle be different, we model them for simplicity with a single exchange constant (J'). All other parameters are taken from the uncoupled Cr_7Ni molecule[21,22]. Gyromagnetic tensors have been fitted to the EPR spectra obtained on isolated Cr_7Ni rings and on the non-interacting Cu complex. The splitting of the low-energy states due to $H^{AC} + H^{BC}$ enables us to extract the value of J' from the low-temperature zero-field Schottky anomaly in the specific heat data; the estimated value is $J'/k_B = -1$ K (see continuous lines in Fig. 2). The detailed splitting pattern of the low-energy levels can be investigated by EPR spectroscopy. The simulated

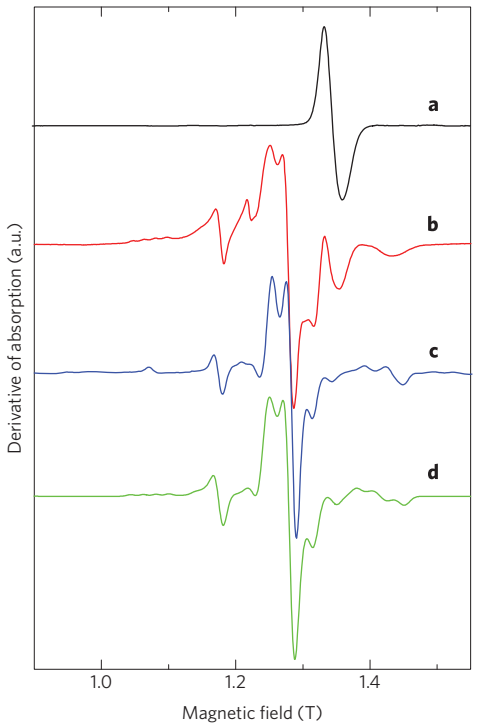

Figure 3 | Powder Q-band EPR spectra of free Cr_7Ni and linked Cr_7Ni–Cu–Cr_7Ni. a,**b**, Measured powder spectra of compounds **2** and **3,** respectively. The experiments were performed at 5 K. **c**, Simulation of spectrum **b** using the microscopic Hamiltonian (equation (1)). **d**, Best fit of spectrum **b** by the effective Hamiltonian (equation (5)), with $J/k_B = -0.44$ K; $D_{ex}/k_B = -0.04$ K; $g_{A,B}$ diagonal tensors with values 1.83(xx), 1.83(yy), 1.79(zz) g_{Cu} diagonal tensor with values 2.27(xx), 2.07(yy), 2.07(zz); Cu hyperfine ($A_{xx} = 2 \times 10^{-2}$ cm^{-1}; A_{yy} and A_{zz} set arbitrarily small at 1×10^{-3} cm^{-1}).

powder spectrum obtained within equation (1) (Fig. 3c) is in good agreement with the experimental data (Fig. 3b).

Because J' is much smaller than the intra-ring exchange constants ($J_i/k_B \approx 20$ K), the low-temperature behaviour of **3** mostly reflects the splitting of the lowest eight levels, and this can be reproduced by an effective three-spin Hamiltonian (see Methods):

$$H = \bar{J} \sum_{i=A,B} \vec{S}_i \cdot \vec{S}_C + \mu_B \vec{B} \cdot \sum_{i=A,B,C} \vec{\vec{g}}_i \cdot \vec{S}_i + D_{ex} \sum_{i=A,B} (2S_{i,z}S_{C,z} - S_{i,x}S_{C,x} - S_{i,y}S_{C,y}). \quad (5)$$

where $\vec{S}_{A,B,C}$ are spin-1/2 operators, $\bar{J}$ is the effective Cu-ring isotropic exchange, $\vec{\vec{g}}_{A,B}$ are the g-tensors of the ring ground doublet, $\vec{\vec{g}}_C = \vec{\vec{g}}_{Cu}$, and D_{ex} is an effective Cu-ring axial exchange resulting from the projection of the rings' dipolar and crystal-field anisotropies (see Methods). The EPR spectrum can be reproduced by equation (5) (Fig. 3d) and is very close to that obtained with the microscopic model described by equation (1). Thus, in spite of its complexity, **3** behaves as three, weakly interacting S = 1/2 centres and in the following we label the low-energy spin configurations of **3** as $|\chi_A, \chi_B, \chi_{Cu}\rangle$, where χ_A, χ_B, $\chi_{Cu} = \uparrow, \downarrow$ represent the z-components of the rings and of Cu total spins.

In compound **4**, in which the link comprises two copper (II) centres (Fig. 1b), the corresponding Hamiltonian for H^C in equation (1) is given by

$$H^C = \vec{B} \cdot (\vec{\vec{g}}_{Cu,1} \cdot \vec{s}_{Cu,1} + \vec{\vec{g}}_{Cu,2} \cdot \vec{s}_{Cu,2}) + J_{Cu,Cu}\vec{s}_{Cu,1} \cdot \vec{s}_{Cu,2}. \quad (6)$$

The analysis of magnetic data of the linking Cu_2 dimer alone gives $J_{Cu,Cu}/k_B = 518$ K (see Supplementary Information, Fig. S3), which makes the dimetallic copper link non-magnetic at low temperature. Therefore, even if the Cu-ring link is identical in **3** and **4**, the two rings are effectively decoupled at low temperature due to the very large and anti-ferromagnetic $J_{Cu,Cu}$. As a consequence, the low-temperature specific heat and the EPR spectra of **4** are identical to those of isolated Cr_7Ni rings (see Supplementary Information, Fig. S2). The same fitting procedure was used to characterize other Cr_7Ni–M–Cr_7Ni derivatives (Table 1; see also Supplementary Information). Together, these results demonstrate the remarkable robustness of Cr_7Ni with respect to chemical linking and show that we can tune the interaction between two well-defined molecular qubits.

Proposal for controlled generation of entangled states

As formalized in equation (5), the Cr_7Ni–Cu–Cr_7Ni system can be regarded as a linear sequence of three weakly coupled qubits belonging to two different species. Such a structure represents a playground for investigating tripartite entanglement in molecular spin qubits. Hereafter, we numerically simulate how different entangled states of the Cr_7Ni–Cu–Cr_7Ni system could be obtained.

Three qubits can be entangled in two fundamentally non-equivalent ways; these correspond to two prototype forms, given by the Greenberger–Horne–Zeilinger (GHZ) and Werner (W) states[28,29]:

$$|GHZ\rangle = (|\uparrow\uparrow\uparrow\rangle + |\downarrow\downarrow\downarrow\rangle)/\sqrt{2},$$
$$|W\rangle = (|\uparrow\uparrow\downarrow\rangle + |\uparrow\downarrow\uparrow\rangle + |\downarrow\uparrow\uparrow\rangle)/\sqrt{3}.$$

In fact, any tripartite entangled state can be converted—with finite probability—into either $|GHZ\rangle$ or $|W\rangle$ by local operations and classical communication[30], whereas it is not possible to convert $|GHZ\rangle$ and $|W\rangle$ into one another by the same means. The GHZ and W states embody diverse aspects of tripartite entanglement, which are captured by different entanglement measurements. In $|W\rangle$, for example, the distance with respect to any classically correlated state (measured by the overall entanglement) is maximum; $|GHZ\rangle$, instead, maximizes the amount of quantum correlations that cannot be expressed in terms of pair-correlations (residual entanglement). The investigation of these two prototypical states is thus fundamental in order to shed light onto the entanglement in such composite molecular systems.

We now show how the state vector $|\Psi(t)\rangle$ of the tripartite system Cr_7Ni–Cu–Cr_7Ni could be driven to both $|GHZ\rangle$ and $|W_{+1/2}\rangle = |W\rangle$ in times much shorter than the expected decoherence time. To this aim, we simulate the dynamics of **3** under the effect of simple electromagnetic pulse sequences. The key ingredients are the specific intermolecular coupling and the resulting level structure of **3**: (i) the $|W\rangle$ states essentially coincide with two eigenstates of the system Hamiltonian whereas GHZ coincide with a linear combination of two of them; (ii) the degeneracy between the required magnetic-dipole transitions is removed by the combined effect of the Cu-ring coupling and of the dipolar and crystal-field anisotropies. The lowest eigenvalues of the spin Hamiltonian described in equation (1) are plotted in Fig. 4a as a function of the magnetic field B_0. At $B_0 = 0.5$ T, for example, the eigenstates $|\Psi_4\rangle$ and $|\Psi_2\rangle$ ($|\Psi_i\rangle$ ordered with increasing energy E_i) correspond with a high degree of approximation to $|W_{+1/2}\rangle$ and $|W_{-1/2}\rangle = (|\uparrow\downarrow\downarrow\rangle + |\downarrow\uparrow\downarrow\rangle + |\downarrow\downarrow\uparrow\rangle)/\sqrt{3}$, whereas $|\Psi_1\rangle$ and $|\Psi_7\rangle$ essentially coincide with the ferromagnetic states $|FM_1\rangle \equiv |\downarrow\downarrow\downarrow\rangle$ and $|FM_2\rangle \equiv |\uparrow\uparrow\uparrow\rangle$, respectively (see Methods). The removed degeneracy in the magnetic dipole transitions connecting the relevant states

Table 1 | Parameters of the effective three-spin Hamiltonian extracted from specific heat, magnetization and EPR data. The anisotropy on the M link is described by an axial term $D_M S_z^2$ where S_z is the *z*-component of the effective spin of the link (column 2).

Metal centre, M	GS spin of M	$J_{ring\text{-}M}/k_B$ (K)	D_M/k_B (K)	g_M
Cu	1/2	−1.0	—	2.27(xx),2.07(yy),2.07(zz)
Cu_2	0	−1.0	—	—
$Ru^{2+}Ru^{3+}$	3/2	0.7	88	2.1

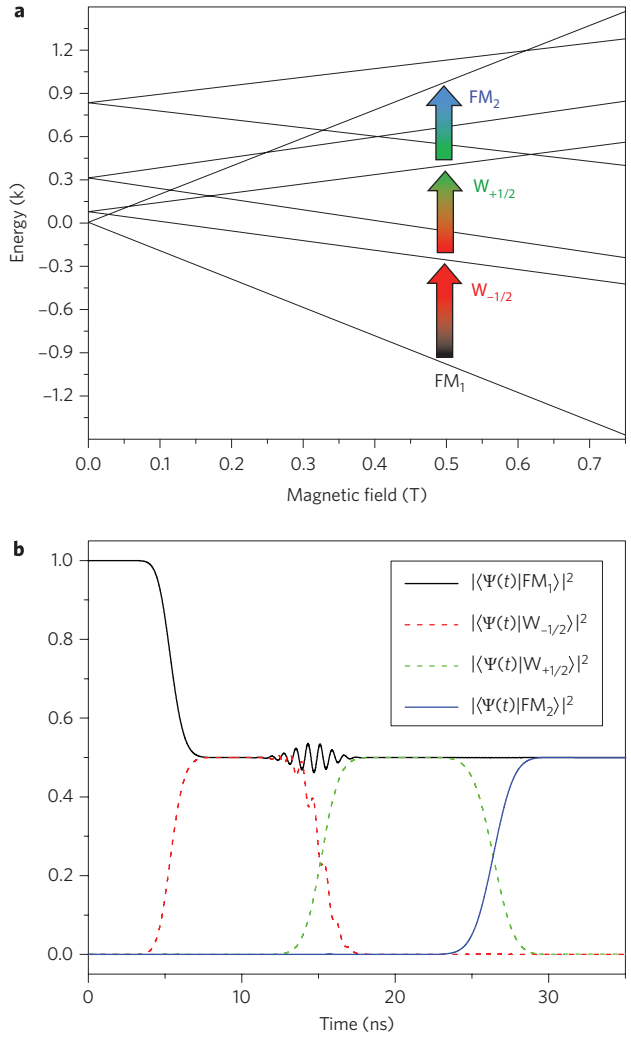

Figure 4 | Simulated generation of GHZ states. a, The lowest energy levels of Cr_7Ni–Cu–Cr_7Ni calculated from equation (1) as a function of a magnetic field B_0 applied along the *z*-axis. The arrows indicate the three sequential transitions used to generate the GHZ state, starting from the system ground state: a first, $\pi/2$ pulse (with $\omega = \omega_{21}$) drives the system to $(|\Psi_1\rangle + |\Psi_2\rangle)/\sqrt{2}$; a second, π pulse ($\omega = \omega_{42}$) induces a population transfer from $|W_{-1/2}\rangle$ to $|W_{+1/2}\rangle$, thus driving the system to $(|\Psi_1\rangle + |\Psi_4\rangle)/\sqrt{2}$; finally, the last π pulse ($\omega = \omega_{74}$) generates the target state $(|\Psi_1\rangle + e^{i\phi}|\Psi_7\rangle)/\sqrt{2} = (|\uparrow\uparrow\uparrow\rangle + e^{i\phi}|\downarrow\downarrow\downarrow\rangle)/\sqrt{2}$. **b**, Simulated time evolution of the eigenstate occupations under the effect of three microwave pulses B_1 along the *x*-axis ($B_0 = 0.5$ T). The pulses have Gaussian time envelope, $B_1(t) = A\exp[-(t-t_i)^2/2\sigma_i^2]$, with $A = 50$ G. The central frequencies, duration and central times are $n_1 = 14.5$ GHz, $n_2 = 13.2$ GHz, $n_3 = 11.6$ GHz, $\sigma_1 = 0.85$ ns, $\sigma_2 = 1.45$ ns, $\sigma_3 = 1.7$ ns, $t_1 = 5$ ns, $t_2 = 15.2$ ns, $t_3 = 26.4$ ns.

($\omega_{12} \neq \omega_{24} \neq \omega_{47}$, where $\hbar\omega_{ij} = E_i - E_j$), allows them to be resolved through pulses much shorter than the expected decoherence times ($T_2 \approx 3$ μs at 2 K)[16]. Therefore, if the system were initially cooled down to the ferromagnetic ground state $|\Psi_1\rangle$, a single resonant π pulse $\boldsymbol{B}_1 = B_1(t)\cos(\omega t)\boldsymbol{x}$ could drive $|\Psi(t)\rangle$ to the eigenstate $|\Psi_2\rangle = |W_{-1/2}\rangle$. To generate a GHZ state, a sequence of three pulses has to be applied to the initial state $|\Psi_1\rangle$. The simulations reported in Fig. 4 demonstrate that the required spectral resolution (which ultimately limits the manipulation rate) allows the GHZ state to be generated in the nanosecond timescale, with realistic values of the pulse amplitude B_1. Possible strategies for the readout of the final states include quantum tomography[30].

One of the next targets comprises using other compounds of the present family for demonstrating a switchable coupling between two molecular qubits (see Fig. 1b). This should be achieved by reversibly driving the linker M from a state where it mediates the magnetic coupling between the rings to another state that suppresses such effective coupling. As a preliminary step in this direction, we consider compound **4**. There, the unit C is frozen in the non-magnetic ground state ($S_C = 0$) by the large antiferromagnetic interaction between the two Cu ions ($J_{Cu,Cu} \gg J'$). Therefore, at low energies, the two Cr_7Ni rings are effectively decoupled. If the Cu_2 dimer could be coherently excited to a ferromagnetic state ($S_C = 1$), an effective coupling between the two rings would be reversibly switched on. This would enable the implementation of unconditional and conditional dynamics (that is, single and two-qubit gates), in spite of the permanent nature of the physical interaction[24,31]. From a practical point of view (transition in the microwave range, reduced phonon generation), it would be preferable to have smaller values of the J_{Cu-Cu} coupling within the Cu dimer. Also, the need for a finite magnetic-dipole transition amplitude between the $S_C = 0$ and $S_C = 1$ states requires a relative tilting of the principal axes of $\vec{\vec{g}}_{Cu1}$ and $\vec{\vec{g}}_{Cu2}$.

Conclusions

In summary, we have experimentally demonstrated that we can control the coupling between molecular spin clusters while preserving the intramolecular interactions of the molecular building blocks. The microscopic description in terms of spin Hamiltonians shows that these complex spin systems can be treated as qubits. Compound **3** meets the requirements for generating maximally entangled tripartite states, and our numerical simulations show how realistic microwave pulse sequences could create GHZ and W states in Cr_7Ni–Cu–Cr_7Ni. Compound **4** is promising with regard to performing single and two-qubit gates in a bipartite system. Further possibilities are created by the ability to vary the link in these systems. For example, the $[Ru^{2+}Ru^{3+}(O_2CCMe_3)_4]^+$ link has a facile one-electron reduction that should allow intermolecular coupling to be controlled through local probes[12]. Overall, this degree of chemical control opens new perspectives for the generation and observation of controlled entanglement in solid-state systems with currently available technologies.

Methods

Full synthetic details are given in the Supplementary Information.

X-ray crystallography. X-ray diffraction data were collected on an Enraf-Nonius FR590 using Mo-K_α-radiation at 150 K. Crystal data for $C_{351}H_{626}Cr_{28}Cu_2F_{32}N_{12}Ni_4O_{142.5}$ (**3**, there are two molecules in the asymmetric unit): triclinic, $P-1$, $a = 16.5633(6)$, $b = 34.1024(10)$, $c = 48.3098(19))$ Å, $\alpha = 83.3020(10)$, $\beta = 87.7560(10)$, $\chi = 90.499(3)^\circ$, $V = 27{,}078.3(17)$ Å^3, $M = 9{,}720.6$, $R_1 = 0.1399$. Crystal data for $C_{208}H_{362}Cr_{14}Cu_2F_{16}N_4Ni_2O_{74}$ (**4**)

monoclinic, $C\,2/c$, $a = 60.9040(8)$, $b = 16.9000(2)$, $c = 30.7200(5)$ Å, $\beta = 103.8030(10)^{\circ}$, $V = 30{,}706.3(7)$ Å^3, $M = 5{,}379.5$, $R_1 = 0.0981$. Crystallographic data (excluding structure factors) for the structures reported in this paper have been deposited with the Cambridge Crystallographic Data Centre as supplementary publication nos. CCDC 689859 and 689860, respectively.

Measurements. Heat capacity measurements were performed using a Quantum Design PPMS system, with ^{3}He system on 1–2 mg pellets of pressed micro-crystals by using the two-tau relaxation methods. Data analysis was carried out by separating the magnetic and lattice contributions. The magnetic contribution is described by the generalized Schottky expression:

$$\frac{C_m}{R} = \beta^2 \frac{\sum_i E_i^2 \exp(-\beta E_i) \sum_i \exp(-\beta E_i) - [\sum_i E_i \exp(-\beta E_i)]^2}{[\sum_i \exp(-\beta E_i)]^2}$$

where the energy levels E_i are eigenvalues of the microscopic spin Hamiltonian (equation (1)).

EPR spectra were measured on a Bruker ESP300E spectrometer; simulations based on equation (1) were performed using a home-made program, whereas simulations based on equation (5) used SIM software (Weihe, H. SIM, University of Copenhagen).

Susceptibility and magnetization measurements were performed using a Quantum Design SQUID system. At low temperature (down to 0.3 K), Hall microprobes were used to measure the magnetic properties on single crystals.

Effective three-spin Hamiltonian. As J' is much smaller than the intra-ring exchange constants ($J_i/J' \approx 20$), the low-energy eigenstates of equation (1) can be reproduced by first-order perturbation theory. This yields an effective three-spin Hamiltonian in which the ground doublet of each ring is described by pseudo-spin 1/2 operators $\vec{S}_A$ and $\vec{S}_B$. In fact, within this doublet the local spin operators $\vec{s}_{i,A}$ and $\vec{s}_{i,B}$ are proportional to pseudo-spin ones: $\vec{s}_{i,A} = \vec{\gamma}_i \vec{S}_A$ and $\vec{s}_{i,B} = \vec{\gamma}_B$, with $\vec{\gamma}_i$ a diagonal matrix, $\gamma_{xx} = \gamma_{yy} \neq \gamma_{zz}$. The structure of $\vec{\gamma}_i$ reflects the axial anisotropy of H_A and H_B, which causes a slight deviation of the ground doublet from a pure $S = 1/2$ state (S-mixing). By expressing the Zeeman term in equation (2) and the Cr and Ni spins in equation (4) in terms of $\vec{S}_A$ and $\vec{S}_B$, equation (5) is obtained with $\bar{J} \approx J'/2$ and $D_{ex} \approx 0.04J'$.

Switchable effective coupling. If the weak ring-link coupling is treated in first-order perturbation theory, the corresponding Hamiltonian for compound **4** in the $S_C = 0$ subspace becomes:
$H^{AC} + H^{BC} = J'(\langle \vec{s}_{Cu,1} \rangle \cdot [\vec{s}_{Cr,A} + \vec{s}_{Ni,A}] + \langle \vec{s}_{Cu,2} \rangle \cdot [\vec{s}_{Cr,B} + \vec{s}_{Ni,B}])$ (see Fig. 1). As $\langle \vec{s}_{Cu,1} \rangle = \langle \vec{s}_{Cu,2} \rangle = 0$, the effective coupling vanishes. This is no longer the case if the Cu_2 dimer is excited to an $S_C = 1$ state.

Numerical procedure. The microscopic spin Hamiltonian described in equation (1) is defined in an N-dimensional Hilbert space, with $N \approx 5 \times 10^9$. In order to calculate the low-E properties we have adopted the following procedure. First, the single-ring Hamiltonians have been diagonalized. Equation (1) has been represented on the product basis $|\phi_A, \phi_B, \phi_C\rangle$, where $|\phi_{A/B}\rangle$ are the eigenstates of the two rings and $|\phi_C\rangle$ are basis vectors for the C link. Because $J' \ll J$, the low-E eigenstates of equation (1) are very well approximated by truncating the product basis to include only the four lowest-lying multiplets of the rings, thus reducing the dimension of the matrix to a manageable value.

It is worth quantifying the degree to which $|\Psi_1\rangle$ $|\Psi_2\rangle$ $|\Psi_4\rangle$ and $|\Psi_7\rangle$ at $B_0 = 0.5$ T (Fig. 4a) match $|FM_1\rangle$, $|W_{-1/2}\rangle$, $|W_{1/2}\rangle$ and $|FM_2\rangle$, respectively. The numerical diagonalization of equation (1) yields that for all four states the deviation is less than 10^{-2}.

Received 5 June 2008; accepted 4 December 2008; published online 1 February 2009

References

1. Nielsen, M. A. & Chuang, I. L. *Quantum Computation and Quantum Information* (Cambridge Univ. Press, 2000).
2. Pan, J.-W., Bouwmeester, D., Daniell, M., Weinfurter, H. & Zeilinger, A. Experimental test of quantum nonlocality in three-photon Greenberger–Horne–Zeilinger entanglement. *Nature* **403,** 515–519 (2000).
3. Zhao, Z. *et al.* Experimental demonstration of five-photon entanglement and open-destination teleportation. *Nature* **430,** 54–58 (2004).
4. Sackett, C. A. *et al.* Experimental entanglement of four particles. *Nature* **404,** 256–259 (2000).
5. Roos, C. F. *et al.* Control and measurement of three-qubit entangled states. *Science* **304,** 1478–1481 (2004).
6. Petta, J. R. *et al.* Coherent manipulation of coupled electron spins in semiconductor quantum dots. *Science* **309,** 2180–2184 (2005).
7. Steffen, M. *et al.* Measurement of the entanglement of two superconducting qubits via state tomography. *Science* **313,** 1423–1425 (2006).
8. Leuenberger, M. & Loss, D. Quantum computing in molecular magnets. *Nature* **410,** 789–793 (2001).
9. Meier, F., Levy, J. & Loss, D. Quantum computing with spin cluster qubits. *Phys. Rev. Lett.* **90,** 047901 (2003).
10. Meier, F., Levy, J. & Loss, D. Quantum computing with antiferromagnetic spin clusters. *Phys. Rev. B* **68,** 134417 (2003).
11. Troiani, F. *et al.* Molecular engineering of antiferromagnetic rings for quantum computation. *Phys. Rev. Lett.* **94,** 207208 (2005).
12. Lehmann, J., Gaita-Ariño, A., Coronado, E. & Loss, D. Spin qubits with electrically gated polyoxometalate molecules. *Nature Nanotech.* **2,** 312–317 (2007).
13. Wernsdorfer, W. Molecular magnets: A long-lasting phase. *Nature Mater.* **6,** 174–176 (2007).
14. Bogani, L. & Wernsdorfer, W. Molecular spintronics using single molecule magnets. *Nature Mater.* **7,** 179–186 (2008).
15. Gatteschi, D., Sessoli, R. & Villain, J. *Molecular Nanomagnets* (Oxford Univ. Press, 2007).
16. Ardavan, A. *et al.* Will spin relaxation times in molecular magnets permit quantum information processing? *Phys. Rev. Lett.* **98,** 057201 (2007).
17. Bertaina, S. *et al.* Quantum oscillations in a molecular magnet. *Nature* **453,** 203–206 (2008).
18. Wernsdorfer, W., Aliaga-Alcalde, N., Hendrickson, D. N. & Christou, G. Exchange-biased quantum tunnelling in a supramolecular dimer of single-molecule magnets. *Nature* **416,** 406–408 (2002).
19. Hill, S., Edwards, R. S., Aliaga-Alcalde, N. & Christou, G. Quantum coherence in an exchange-coupled dimer of single-molecule magnets. *Science* **302,** 1015–1018 (2003).
20. Larsen, F. K. *et al.* Synthesis and characterization of heterometallic $\{Cr_7M\}$ wheels. *Angew. Chem. Int. Ed.* **42,** 101–105 (2003).
21. Carretta, S. *et al.* Topology and spin dynamics in magnetic molecules. *Phys. Rev. B* **72,** 060403 (2005).
22. Caciuffo, R. *et al.* Spin dynamics of heterometallic Cr_7M wheels (M = Mn, Zn, Ni) probed by inelastic neutron scattering. *Phys. Rev. B* **71,** 174407 (2005).
23. Carretta, S. *et al.* Quantum oscillations of the total spin in a heterometallic antiferromagnetic ring: evidence from neutron spectroscopy. *Phys. Rev. Lett.* **98,** 167401 (2007).
24. Troiani, F., Affronte, M., Carretta, S., Santini, P. & Amoretti, G. Proposal for quantum-gate in permanently coupled AF spin rings, without need of local fields. *Phys. Rev. Lett.* **94,** 190501 (2005).
25. Troiani, F., Bellini, V. & Affronte, M. Decoherence induced by hyperfine interactions with nuclear spins in antiferromagnetic molecular rings. *Phys. Rev. B* **77,** 054428 (2008).
26. Corradini, V. *et al.* Isolated heterometallic Cr_7Ni rings grafted on Au(111) surface. *Inorg. Chem.* **46,** 4937–4943 (2007).
27. Affronte, M. *et al.* Linking rings through diamines and clusters: exploring synthetic methods for making magnetic quantum gates. *Angew. Chem. Int. Ed.* **44,** 6496–6500 (2005).
28. Dür, W., Vidal, G. & Cirac, J. I. Three qubits can be entangled in two inequivalent ways. *Phys. Rev. A* **62,** 062314 (2000).
29. Röthlisberger, B., Lehmann, J., Saraga, D. S., Traber, P. & Loss, D. Highly entangled ground states in tripartite qubit systems. *Phys. Rev. Lett.* **100,** 100502 (2008).
30. Laflamme, R., Knill, E., Zurek, W. H., Catasti, P. & Mariappan, S. V. S. NMR Greenberger–Horne–Zeilinger states. *Phil. Trans. R. Soc. Lond. A* **356,** 1941–1948 (1998).
31. Carretta, S., Santini, P., Amoretti, G., Troiani, F. & Affronte, M. Spin triangles as optimal units for molecule-based quantum gates. *Phys. Rev. B* **76,** 024408 (2007).

Acknowledgements

This work was supported by the European Community through the Network of Excellence Molecular Approach to Nanomagnets and Multifunctional Materials (MAGMANet), contract N.515767 and the ICT-FET Open Project Molecular Spin Clusters for Quantum Information Processes (MolSpinQIP), contract N. 211284, by the Engineering and Physical Sciences Research Council (EPSRC) (UK), and by Progetti di Interesse Nazionale (PRIN) 2006029518 (IT). F.T. (Modena) was supported by Fondo per gli Investimenti della Ricerca di Base (FIRB) Contract RBIN01EY74.

Author contributions

The key idea to use Cr_7Ni spin systems for quantum processes was jointly developed by the Manchester, Modena and Parma leaders. F. Troiani, S.C., P.S. and G.A. contributed with modelling, numerical simulations and development of quantum schemes. A.G. and A.C. performed specific heat and magnetic measurements; in addition to these, M.A. contributed with data analysis. G.T. made the compounds after discussion with R.E.P.W. F. Tuna measured the EPR spectra and susceptibility, and E.J.L.M. performed the EPR simulations. The X-ray structure determinations were performed by R.J.P. and C.A.M.

Additional information

Supplementary Information accompanies this paper at www.nature.com/naturenanotechnology. Reprints and permission information is available online at http://npg.nature.com/reprintsandpermissions/. Correspondence and requests for materials should be addressed to M.A. and R.E.P.W.